crystals

MDPI

Article

Impact of the Liquid Crystal Director Twisting on Two-Beam Energy Exchange in a Hybrid Photorefractive Inorganic-Liquid Crystal Cell

Victor Yu. Reshetnyak [1], Igor P. Pinkevych [1,*], Michael E. McConney [2], Jonathan E. Slagle [2] and Dean R. Evans [2]

[1] Physics Faculty, Taras Shevchenko National University of Kyiv, 01601 Kyiv, Ukraine; VReshetnyak@univ.kiev.ua

[2] Air Force Research Laboratory, Materials and Manufacturing Directorate, Wright-Patterson Air Force Base, OH 45433, USA; Michael.McConney.1@us.af.mil (M.E.M.); jonathan.slagle.2@us.af.mil (J.E.S.); dean.evans@us.af.mil (D.R.E.)

* Correspondence: ipinkevych@gmail.com

Received: 31 October 2020; Accepted: 1 December 2020; Published: 3 December 2020

check for updates

Abstract: We studied the energy transfer between light beams on the director grating in a hybrid photorefractive liquid crystal (LC) cell assuming the propagation of light waves in the cell to be in the Mauguin regime. This approach makes it possible to trace the change of the gain coefficient dependence on the director grating spacing with the change of the LC director twist. Conditions for the LC flexoelectric parameters and the director helix pitch necessary for transformation the gain coefficient dependence from the nematic to cholesteric type are obtained. The influence of the director splay and bend deformations on the gain coefficient is also studied.

Keywords: liquid crystal; hybrid photorefractive cell; director grating; two-beam energy exchange

1. Introduction

In recent years, a strong two-beam energy transfer between light beams coupled on the refractive index grating has been observed in liquid crystals (LCs). The high modulation of the refractive index of the order of 0.2, obtained due to LC director reorientation, made it possible to increase the intensity of one of the beams with a gain coefficient almost two orders of magnitude greater than in solid photorefractive crystals [1–6].

In a scheme with a hybrid organic–inorganic cell a LC layer is placed between two solid substrates, one or two of which is photorefractive. The incident intersecting coherent light beams interfere and generate space charges in the inorganic photorefractive substrate(s). The space charges create a spatially periodic electric field, which penetrates the LC layer and modulates the LC director. The resulting director grating induces the refractive index grating and ensures coupling of the intersecting beams propagating in the LC [7–11]. When discussing the mechanism of director reorientation in hybrid systems, the space-charge field couples with the director through an interaction with the LC flexoelectric polarization [12–14] rather than through the LC static dielectric anisotropy [15,16]. The description of the experimental results obtained for both nematic [12] and cholesteric LC cells [13,14] required an additional assumption whereby the director magnitude is a nonlinear function of the space-charge field. This leads to the replacement of the flexoelectric coefficients by their effective values, which depend on the space-charge field. Possible physical mechanisms of this nonlinearity are discussed in [12]. Despite the fact that the physical mechanism of interaction of the space-charge field with the director is the same for nematic and cholesteric LCs, the observed dependence of the gain coefficient of the incident signal beam on the director grating spacing is very different. The gain coefficient is defined as

$\Gamma = \frac{1}{L}\ln\left|A_1(out)/A_1(in)\right|^2$, where $A_1(in)$ and $A_1(out)$ are the amplitudes of the signal beam at the input and output of the LC cell, respectively, L is a cell thickness. Typical dependences of the signal beam gain coefficient on the director grating spacing in hybrid cells with nematic and cholesteric LCs are shown in Figure 1a,b, respectively [12,14].

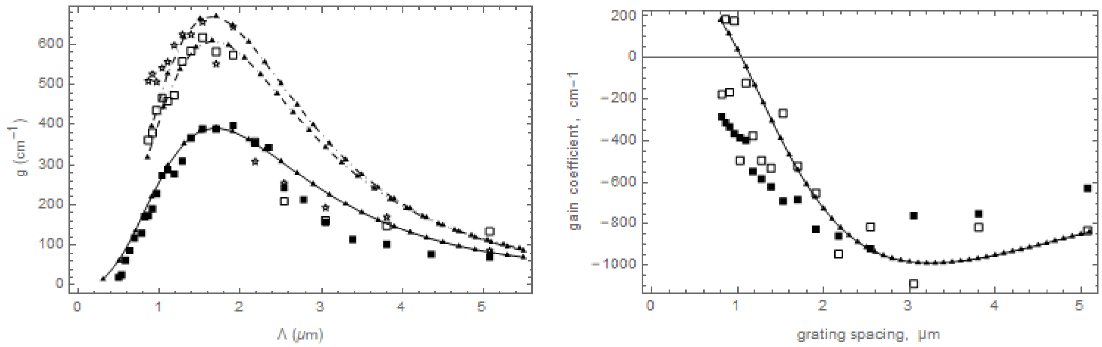

(**a**) (**b**)

Figure 1. Typical dependence of the signal beam gain coefficient on the grating spacing in hybrid organic-inorganic cells with LC. (**a**) nematic LC, g is the gain coefficient, Λ is the grating spacing; theoretical fit for the gain coefficient (solid and dashed lines) to experimental data for nematic LC TL205 cells of different thickness: L (μm) = 5.7—stars, 7.1—light boxes, 10—black boxes [12]; (**b**) cholesteric LC mixture BL038/CB15, theoretical results – curve, experimental data—boxes, the cell thickness $L = 5$ μm [14].

There are two possible explanations for this difference: (1) the character of electromagnetic wave propagation in nematic and cholesteric LCs (and, therefore, the character of the interaction of waves) is different, and (2) the parameters that determine the director grating in nematic and cholesteric LCs differ significantly. To study this problem, we consider the energy transfer between light beams in hybrid photorefractive LC cells with different director twisting, but the same character of electromagnetic wave propagation through the cell. This condition may be realized in the so-called Mauguin regime, when the wave polarization follows the LC director [17]. In this case, we can trace the change in the gain coefficient when changing the LC director twisting from a nematic to a cholesteric type without changing the character of wave propagation.

The paper is organized as follows. In Section 2 we introduce the model of a hybrid LC cell placed in the interference pattern of two incident light beams, and obtain expressions for the director angles under the photorefractive field. In Section 3 we consider the light beams propagation in the Mauguin regime and derive an expression for the signal beam gain coefficient. Results of numerical calculations of the gain coefficient and their discussion are presented in Section 4. In Section 5 we present some brief conclusions.

2. Model and CLC Director

Consider a hybrid cell with the z-axis directed perpendicular to the cell planes. The cholesteric liquid crystal (CLC) is bound by the substrates at $z = -L/2$ and $z = L/2$, where L is a CLC layer thickness (see Figure 2). The entrance substrate is a photorefractive crystal, and the exit substrate is glass (non-photorefractive). The hybrid cell is illuminated by two intersecting polarized coherent light beams $\mathbf{E}_1 = A_1\mathbf{e}_1\exp(i\boldsymbol{k}_1\boldsymbol{r} - i\omega t)$ and $\mathbf{E}_2 = A_2\mathbf{e}_2\exp(i\boldsymbol{k}_2\boldsymbol{r} - i\omega t)$. The wave vectors of the light beams, $\boldsymbol{k}_1$ and $\boldsymbol{k}_2$, are symmetric with regard to the cell normal, so that the incidence angles are equal. On the entrance plane $z = -L/2$ the CLC director and the polarization vectors of the beams, $\mathbf{e}_1$ and $\mathbf{e}_2$, lie in the xz-plane. However, as the beams propagate across the CLC cell in the Mauguin regime, the polarization vectors of the beams rotate following the CLC director.

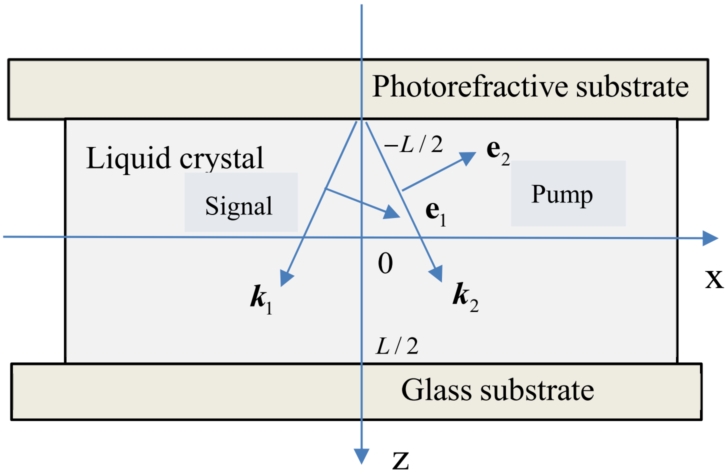

Figure 2. Schematic of the cholesteric liquid crystal (CLC) cell, showing light beams incident from photorefractive medium, together with associated wave and polarization vectors. $\alpha_1,\ \alpha_2$ are the angles of propagation of light beams in the CLC ($\alpha_1 = \alpha_2 \equiv \alpha$).

The beams produce a light intensity interference pattern in the photorefractive substrate for, $z \leq -L/2$,

$$I(x) = (I_1 + I_2)\left[1 + \frac{1}{2}(m\ \exp(iqx) + c.c.)\right] \tag{1}$$

where $m = 2\ \cos(2\delta)A_1 A_2^*/(I_1 + I_2)$ is the modulation parameter, and 2δ is the angle between incident beams in the photorefractive medium, $I_1 = A_1 A_1^*$, $I_2 = A_2 A_2^*$ are the intensities of incident beams, and $q = k_{1x} - k_{2x} = 2k \sin\delta$ is the wave number of the intensity pattern.

The light intensity pattern given by Equation (1) induces a space-charge field inside the photorefractive substrate, which is modulated along the x-axis with a period equal to $\Lambda = 2\pi/q$. This field penetrates the CLC and reorients the CLC director. It is convenient to present the CLC director in the form $\mathbf{n} = (\cos\varphi(x,z)\cos\vartheta(x,z),\ \sin\varphi(x,z)\cos\vartheta(x,z), \sin\vartheta(x,z))$ where $\vartheta(x,z)$ is the director polar angle with respect to the xy-plane and $\varphi(x,z)$ is the director azimuth angle with respect to the x-axis. Taking into account the spatial periodicity of the photorefractive field along the x-axis we can present the polar and azimuthal director angles in the form

$$\begin{aligned} \vartheta(x,z) &= \theta_0(z) + [\theta(z)\exp(iqx) + c.c.], \\ \varphi(x,z) &= \varphi_0(z) + [\varphi(z)\exp(iqx) + c.c.], \end{aligned} \tag{2}$$

where $\varphi_0(z) = \frac{2\pi}{p}(z + L/2)$ and p is the cholesteric pitch.

The director spatial profile can be found by minimizing the total free energy functional of the CLC cell, $F = F_{el} + F_l + F_E + F_{fl}$, where

$$\begin{aligned} F_{el} &= \tfrac{1}{2}\int\Big[K_{11}(\nabla\cdot\mathbf{n})^2 + K_{22}(\mathbf{n}\cdot\nabla\times\mathbf{n} + 2\pi/p)^2 + K_{33}(\mathbf{n}\times\nabla\times\mathbf{n})^2\Big]\,dV, \\ F_l &= -\tfrac{\varepsilon_0\varepsilon_a}{4}\int(\mathbf{n}\cdot\mathbf{E}_{hv})^2 dV,\ F_E = -\tfrac{\varepsilon_0\tilde{\varepsilon}_a}{2}\int(\mathbf{n}\cdot\mathbf{E})^2 dV,\ F_{fl} = -\int\Big(\mathbf{P}_f\cdot\mathbf{E}\Big)\,dV. \end{aligned} \tag{3}$$

Here F_{el} is the CLC bulk elastic energy, F_l is the contribution of the light field $\mathbf{E}_{hv}$, F_E is the contribution from the photorefractive electric field $\mathbf{E}$ penetrating the CLC cell from the photorefractive substrate, and F_{fl} is the contribution from the interaction of the photorefractive field with the CLC flexoelectric polarization $\mathbf{P}_f = e_1\mathbf{n}\nabla\cdot\mathbf{n} + e_3(\nabla\times\mathbf{n}\times\mathbf{n})$; $\mathbf{n}$ is a director, and $e_1,\ e_3$ are the flexoelectric coefficients, and $\tilde{\varepsilon}_a,\ \varepsilon_a$ are the CLC static dielectric anisotropy and dielectric anisotropy at optical frequency, respectively.

In hybrid photorefractive–LC systems, the LC dielectric anisotropy term F_E can be neglected with respect to the LC flexopolarization term F_{fl} [12]. The light field contribution F_l can be neglected because the CLC dielectric anisotropy at optical frequency $\varepsilon_a << 1$. For simplicity, we will also suppose the one elastic constant approximation, $K_{11} = K_{22} = K_{33} = K$. Then, substituting Equation (2) and expression for the photorefractive electric field **E** (see [14]) into Equation (3) we can obtain the linearized Euler–Lagrange equations for the angles $\theta(z)$, $\varphi(z)$ and $\theta_0(z)$:

$$\frac{\partial^2\theta}{\partial z^2} - \left(q^2 + g^2\right)\theta = r_1\left[iq\cos\varphi_0 E_{0z} + \left(\frac{\partial E_{0z}}{\partial z} - iq\cos^2\varphi_0 E_{0x}\right)\theta_0\right] - r_2 g\sin\varphi_0 E_{0x} \tag{4}$$

$$\frac{\partial^2\varphi}{\partial z^2} - q^2\varphi = -iqr_1\left(\frac{1}{2}\sin 2\varphi_0 E_{0x} + \theta_0\sin\varphi_0 E_{0z}\right) + r_2\sin\varphi_0\frac{\partial\theta_0}{\partial z}E_{0x} \tag{5}$$

$$\frac{\partial^2\theta_0}{\partial z^2} - g^2\theta_0 = 0 \tag{6}$$

where E_{0x}, E_{0z} are the Cartesian components of the photorefractive field, $r_1 = (e_1 + e_3)/K$, $r_2 = (e_1 - e_3)/K$ and $g = 2\pi/p$.

Equations (4)–(6) were derived previously [14], but solved only for the case of the waveguide regime when the eigenmodes in CLC are nearly circular and the condition $\lambda > p\,(n_e - n_0)$ holds, where λ is the free space wavelength and n_0, n_e are the CLC ordinary and extraordinary wave refraction indices, respectively. In this work, we solve Equations (4)–(6) for the Mauguin regime, when the opposite condition is fulfilled, i.e., $\lambda < p\,(n_e - n_0)$ [17]. Neglecting small terms of order e^{-qL}, solutions obtained are as follows,

$$\theta_0(z) = \frac{\theta_{02}\sinh[g(z + L/2)] - \theta_{01}\sinh[g(z - L/2)]}{\sinh gL}, \tag{7}$$

$$\theta(z) = \theta(-L/2)d(z) \tag{8}$$

where

$$\theta(-L/2) = \frac{1}{2}E_{sc}(q)\tilde{q}m\,\frac{r_1(\tilde{q}^2 - q^2 - 2g^2) + 2r_2g^2}{\left(\tilde{q}^2 - q^2 - 2g^2\right)^2 + 4\tilde{q}^2g^2}, \tag{9}$$

$$\begin{aligned} d(z) = {} & e^{-\sqrt{q^2+g^2}(z+L/2)} + \left(2e^{-\tilde{q}L}\cos gL - e^{-\sqrt{q^2+g^2}L}\right)e^{\sqrt{q^2+g^2}(z-L/2)} \\ & -2e^{\tilde{q}(z-3L/2)}\cos[g(z + L/2)] \end{aligned} \tag{10}$$

Here $E_{sc}(q)$ is the space-charge electric field, $\tilde{q} = q\sqrt{\left(\tilde{\varepsilon}_\parallel + \tilde{\varepsilon}_\perp\right)/2\tilde{\varepsilon}_\perp}$, $\tilde{\varepsilon}_\parallel$ and $\tilde{\varepsilon}_\perp$ are the components of the CLC low frequency dielectric tensor along and perpendicular to the director, and θ_{01}, θ_{02} are the director pretilt angles in the xz-plane on the CLC cell substrates $z = -L/2$ and $z = L/2$, respectively. As will be stated below, the azimuth angle $\varphi(z)$ makes a negligibly small contributions to the gain and therefore is not presented here due to its cumbersome nature.

3. Beam Coupling and Gain

Using obtained Equations (7)–(10) for the director angles, we can write the CLC optical frequency dielectric tensor $\varepsilon_{ij} = \varepsilon_\perp\delta_{ij} + \varepsilon_a n_i n_j$, which takes the form

$$\hat{\varepsilon}(x,z) = \hat{\varepsilon}_1(z) + \hat{\varepsilon}_2(z) + [\hat{\varepsilon}_3(z)\exp(iqx) + c.c.] \tag{11}$$

Here the first term in Equation (11) corresponds to a CLC with zero director pretilt on the cell boundaries. The second term takes into account the director profile induced by the nonzero director pretilt on the cell boundaries. The third term describes the dielectric tensor modulation due to the director modulation by the spatially periodic photorefractive field.

The expression for $\hat{\varepsilon}_3(z)$ in the third term of Equation (11) is as follows [14],

$$\hat{\varepsilon}_3 = \varepsilon_a \theta(z) \begin{vmatrix} -2\theta_0 \cos^2\varphi_0 & -\theta_0 \sin 2\varphi_0 & \cos\varphi_0 \\ -\theta_0 \sin 2\varphi_0 & -2\theta_0 \sin^2\varphi_0 & \sin\varphi_0 \\ \cos\varphi_0 & \sin\varphi_0 & 2\theta_0 \end{vmatrix} + \varepsilon_a \varphi(z) \begin{vmatrix} -\sin 2\varphi_0 & \cos 2\varphi_0 & -\theta_0 \sin\varphi_0 \\ \cos 2\varphi_0 & \sin 2\varphi_0 & \theta_0 \cos\varphi_0 \\ -\theta_0 \sin\varphi_0 & \theta_0 \cos\varphi_0 & 0 \end{vmatrix} \quad (12)$$

where $\varepsilon_a = \varepsilon_{\|} - \varepsilon_{\perp}$, and $\varepsilon_{\|}$, $\varepsilon_{\perp}$ are the principal values of the dielectric tensor at the optical frequency. Formulas for $\hat{\varepsilon}_1(z)$, $\hat{\varepsilon}_2(z)$ are not important here but are presented in paper [14].

The electric field of the light beams must satisfy the vector wave equation

$$\nabla \times \nabla \times \mathbf{E}_{hv} - \frac{\omega^2}{c^2}\hat{\varepsilon}(x,z)\mathbf{E}_{hv} = 0 \quad (13)$$

where the dielectric permittivity is described by Equation (11), $\mathbf{E}_{hv} = \mathbf{E}_1 + \mathbf{E}_2$, $\mathbf{E}_1$ and $\mathbf{E}_2$ are the electric vectors of the light beams.

Neglecting reflection of the waves from the far side of the cholesteric cell, we start solving Equation (13) in a zeroth order approximation substituting $\hat{\varepsilon}(x,z) = \hat{\varepsilon}_1(z) + \hat{\varepsilon}_2(z)$. In this approximation, the electric vectors of the waves, $\mathbf{E}_1 = \mathbf{E}_1^0$ and $\mathbf{E}_2 = \mathbf{E}_2^0$, separately obey the wave equation with dielectric tensor $\hat{\varepsilon}_1(z) + \hat{\varepsilon}_2(z)$. As shown in paper [14], the contribution from $\hat{\varepsilon}_2(z)$ is small and in the Mauguin regime, $\lambda < p\ (n_e - n_0)$, the wave equation has a solution when the electric field vector of the light beam follows the liquid crystal director. In this case, for small angles α, the electric field vector components of both light beams can be written in the form

$$\begin{aligned} E_{1x}^0 &= A_1 \cos\varphi_0 e^{i[(\omega/c)n_e(z+L/2)+k_{1x}x]}, \\ E_{1y}^0 &= A_1 \sin\varphi_0 e^{i[(\omega/c)n_e(z+L/2)+k_{1x}x]}, \\ E_{1z}^0 &= i\alpha \frac{n_e c}{\varepsilon_\perp \omega}\frac{\partial E_{1x}^0}{\partial z} - \theta_0(z)\frac{\varepsilon_a}{\varepsilon_\perp}(\cos\varphi_0 E_{1x}^0 + \sin\varphi_0 E_{1y}^0) \end{aligned} \quad (14)$$

and

$$\begin{aligned} E_{2x}^0 &= A_2 \cos\varphi_0 e^{i[(\omega/c)n_e(z+L/2)+k_{2x}x]}, \\ E_{2y}^0 &= A_2 \sin\varphi_0 e^{i[(\omega/c)n_e(z+L/2)+k_{2x}x]}, \\ E_{2z}^0 &= -i\alpha \frac{n_e c}{\varepsilon_\perp \omega}\frac{\partial E_{2x}^0}{\partial z} - \theta_0(z)\frac{\varepsilon_a}{\varepsilon_\perp}(\cos\varphi_0 E_{2x}^0 + \sin\varphi_0 E_{2y}^0) \end{aligned} \quad (15)$$

Taking into account the third term of Equation (11) the coupling between light waves appears in Equation (13). In this case, we follow a procedure first outlined by Kogelnik [18], which used in our previous related papers [12–14]. According to this procedure we can seek $\mathbf{E}_1$ and $\mathbf{E}_2$ in the form of Equations (14) and (15) setting the electric field magnitudes $A_1 = A_1(z)$, $A_2 = A_2(z)$, and allowing them to vary slowly across the cell. We will consider beam 1 as a signal, and beam 2 as a pump, adopting the undepleted pump approximation [19], for which the pump magnitude $|A_2| >> |A_1|$. In this case, the signal has a negligible effect on the pump magnitude, which may be regarded as constant, and the set of coupled equations for magnitudes $A_1(z)$ and $A_2(z)$ reduces after some algebra to the single equation

$$\left(E_{1x}^{0*}\frac{\partial}{\partial z}E_{1x}^0 + E_{1y}^{0*}\frac{\partial}{\partial z}E_{1y}^0\right)\frac{\partial}{\partial z}A_1(z) = -\frac{\omega^2}{2c^2}A_1(z)\ \mathbf{E}_1^{0*}\hat{\varepsilon}_3\mathbf{E}_2^0 e^{iqx} \quad (16)$$

Using Equations (14) and (15) for, $\mathbf{E}_1^0$, $\mathbf{E}_2^0$ and Equation (12) for $\hat{\varepsilon}_3$ we obtain that expression $\mathbf{E}_1^{0*}\hat{\varepsilon}_3\mathbf{E}_2^0 e^{iqx}$ on the right side of Equation (16), which reduces to

$$\mathbf{E}_1^*\hat{\varepsilon}_3\mathbf{E}_2 e^{iqx} = 2A_1(z)A_2\varepsilon_a\theta(z)\left(-\theta_0\frac{\varepsilon_{\|}}{\varepsilon_\perp} + i\alpha\frac{n_e}{\varepsilon_\perp}\frac{\lambda}{p}\sin\varphi_0\right) \quad (17)$$

As a result, Equation (16) takes the following form:

$$\frac{\partial}{\partial z}A_1(z) \;=\; -i\frac{\omega}{c}A_2\frac{\varepsilon_a}{\varepsilon_\perp}n_e\theta(z)\left[\theta_0(z) - i\alpha\frac{\lambda}{n_e p}\sin\varphi_0(z)\right] \tag{18}$$

As we can see from Equation (18), in the Mauguin regime the azimuth angle $\varphi(z)$ does not give contribution to coupling of the signal beam with the pump. Furthermore, in the Mauguin regime $\lambda < p\ (n_e - n_0)$, the second term in brackets is at least an order of magnitude less than the first term and therefore can be omitted. Neglecting this term, we can write the solution to Equation (18) as follows

$$A_1(z) \approx A_1(-L/2) - i\frac{\omega}{c}\frac{\varepsilon_a}{\varepsilon_\perp}n_e A_2\int\limits_{-L/2}^{z}\theta_0(z)\theta(z)\,dz \tag{19}$$

The signal beam gain in the CLC layer is defined as

$$G \;=\; \left|\frac{A_1(L/2)}{A_1(-L/2)}\right|^2 \tag{20}$$

where after substituting Equation (8) in Equation (19)

$$A_1(L/2) \;=\; A_1(-L/2) - i\frac{\omega}{c}\frac{\varepsilon_a}{\varepsilon_\perp}n_e\theta(-L/2)A_2\int\limits_{-L/2}^{L/2}\theta_0(z)d(z)\,dz \tag{21}$$

Substituting Equation (9) into Equation (21) we take into account that in the undepleted pump approximation, $m \approx 2\ \cos(2\delta)A_1(-L/2)/A_2$. This yields the following result for the signal beam gain

$$G \;=\; \left|1 - iE_{sc}(q)\tilde{q}\frac{\omega}{c}\frac{\varepsilon_a}{\varepsilon_\perp}n_e\cos(2\delta)\frac{r_1(\tilde{q}^2 - q^2 - 2g^2) + 2r_2g^2}{(\tilde{q}^2 - q^2 - 2g^2)^2 + 4\tilde{q}^2g^2}\int\limits_{-L/2}^{L/2}\theta_0(z)d(z)\,dz\right|^2 \tag{22}$$

Using Equations (7) and (10) we can calculate the integral in Equation (22). The result expressed in terms of the exponential gain coefficient is as follows:

$$\begin{gathered}\Gamma \;=\; \tfrac{1}{L}\ln|G| \;=\; \tfrac{1}{L}\ln\left|1 - \tfrac{2\pi n_e}{\lambda}\tfrac{n_e^2-n_o^2}{n_o^2}\tfrac{iE_{sc}(q)\cos(2\delta)}{2\sinh gL[(\tilde{q}^2-q^2-2g^2)^2+4\tilde{q}^2g^2]}\cdot\right. \\ \left.\left\{\tilde{q}b\left(\tfrac{\theta_{01}e^{gL}-\theta_{02}}{\sqrt{q^2+g^2}+g} - \tfrac{\theta_{01}e^{-gL}-\theta_{02}}{\sqrt{q^2+g^2}-g}\right) + [g^2c + \tilde{q}b(\tilde{q}-g)]\left[\tfrac{(\theta_{01}e^{-gL}-\theta_{02})}{(\tilde{q}-g)^2+g^2} - \tfrac{(\theta_{01}e^{gL}-\theta_{02})}{(\tilde{q}+g)^2+g^2}\right]\right\}\right|^2,\end{gathered} \tag{23}$$

where

$$b \;=\; r_1(\tilde{q}^2 - q^2 - 2g^2) + 2r_2g^2,\; c \;=\; r_2(\tilde{q}^2 - q^2 - 2g^2) - 2r_1\tilde{q}^2 \tag{24}$$

4. Numerical Calculations and Discussions

For calculations, we use the expression for the space-charge field $E_{sc}(p)$ obtained in an infinite photorefractive medium for a diffusion-dominated case [19,20]:

$$E_{sc}(q) \;=\; \frac{iE_d}{1 + \frac{E_d}{E_q}},\; E_d \;=\; q\frac{k_bT}{e},\; E_q \;=\; \left(1 - \frac{N_a}{N_d}\right)\frac{eN_a}{\varepsilon_0\varepsilon_{Ph}q} \tag{25}$$

where E_d is the diffusion field, E_q is the so-called saturation field, N_a and N_d are respectively the acceptor and donor impurity densities, ε_{Ph} is the dielectric permittivity of photorefractive material, and e is the electron charge. In order to evaluate $E_{sc}(q)$, we follow Reference [7], where the ratio of the acceptor to donor impurity densities is estimated to be very small, i.e., $N_d >> N_a$, with $N_a \approx 3.8 \cdot 10^{21}$ m^{-3} and the dielectric permittivity of the photorefractive layer equals to $\varepsilon_{Ph} = 200$ at temperature $T = 300$ K.

Typical parameters for experiments with hybrid photorefractive cells are: the wavelength of the incident light beams, $\lambda = 532$ nm; the CLC cell thickness, $L = 10$ µm; and the director pretilt angles at the CLC cell substrates, $\theta_{01} = 12°$, $\theta_{02} = -12°$. In the case of the Mauguin regime, the CLC pitch is comparable to the cell thickness. Such a situation takes place for nematic LC twisted due to the boundary conditions or doped with a small concentration of the chiral agent. For numerical calculations, we take a nematic LC TL208 supposing that it can contain a small concentration of some chiral agent providing the necessary twisting. The LC TL208 ordinary and extraordinary refractive indices are $n_o = 1.527$ and $n_e = 1.744$, respectively, and the low-frequency dielectric constants are $\tilde{\varepsilon}_{\|} = 9.1$ and $\tilde{\varepsilon}_{\perp} = 4.1$ [12]. These experimental parameters provide an estimate of the possible values of the cholesteric pitch satisfying the condition of the Mauguin regime at $p > 2.45$ µm.

Replacing the flexoelectric parameters r_1 and r_2 by their effective values, we use the phenomenological expression $r_{i,ef} = r_i\left(1 + \mu q^2 |E_{sc}|^2\right)$ proposed in paper [12] with the fitting parameter $\mu = 2 \cdot 10^{-21}$ J^{-2}C^{2}m^4 estimated in [12] for the LC TL208. The values of parameters r_1 and r_2 are not known for TL208, however, they were measured in other LCs [21–24]. A value of the order of 1 Cm$^{-1}N^{-1}$ can be regarded as typical for the absolute values of the above flexoelectric parameters.

In Figure 3, we show the dependence of the gain coefficient on the director grating spacing $\Lambda = 2\pi/q$ for different values of the director helix pitch at the different values of the flexoelectric parameter r_2 keeping the flexoelectric parameter r_1 unchanged. When the director helix pitch is large enough (for example, $p = 2L$ as in Figure 3a), the gain coefficient dependence on the director grating spacing has a nematic type (i.e., the gain coefficient has positive values in the entire range of Λ as, for example, seen in Figure 1a) for all values of the flexoelectric parameter r_2. Decreasing of the helix pitch leads to the change of the gain coefficient behavior from the nematic type to the cholesteric type (that is, with increasing Λ, negative values appear with a minimum), but only when the parameter r_2 is negative (compare Figure 3a,b with Figure 3c,d).

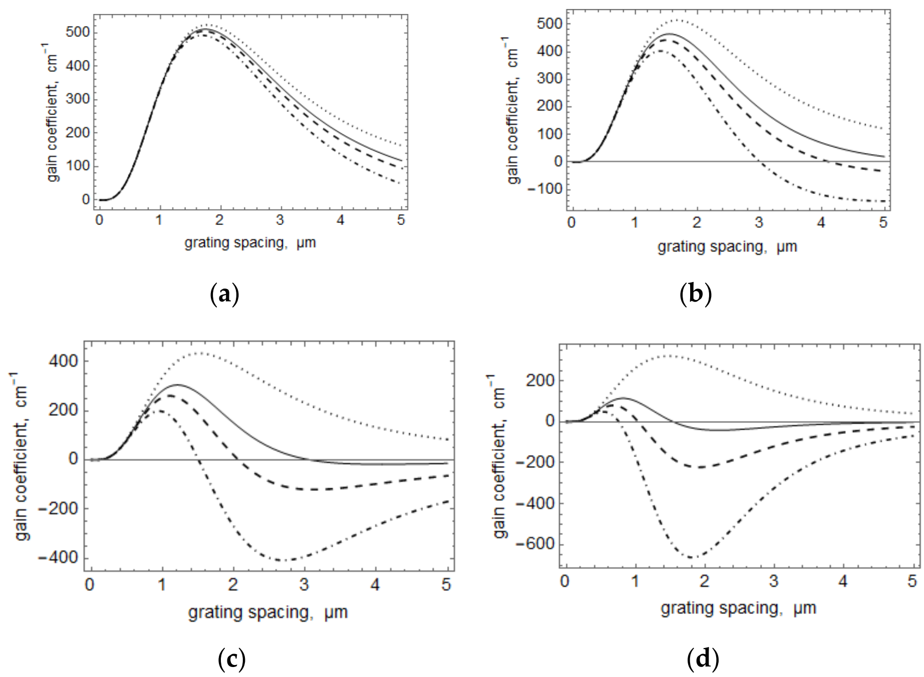

Figure 3. Gain coefficient versus grating spacing for different values of the director helix pitch: (**a**) $p = 2L$, (**b**) $p = L$, (**c**) $p = L/2$, (**d**) $p = L/4$; $r_2 = 2$ (dotted), 0 (solid), −1 (dashed), −3 (dot-dashed); $r_1 = 1$.

As the calculations show, for a large director helix pitch such that $p > 2L$ the value of the pitch does not practically influence the gain coefficient value for all reasonable values of the parameter r_2. In this case, the influence of the parameter r_2 on the gain coefficient becomes negligibly small and the gain coefficient depends only on the flexoelectric parameter r_1. This agrees with the results of the paper [12], where it is shown that the gain in the hybrid nematic LC cells depends only on the parameter r_1.

Influence of the flexoelectric parameter r_1 on the gain coefficient for the cases $p = L$ and $p = L/4$ is shown in Figure 4a,b, respectively. For both the nematic and cholesteric types of the gain behavior, a change of the parameter r_1 does not change the character of the gain coefficient dependence on the grating spacing. However, extremes of the gain coefficient increase with an increase of r_1.

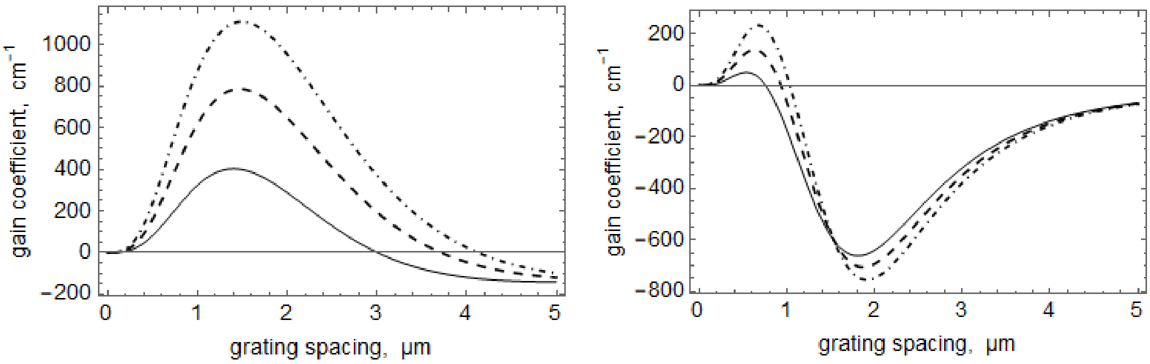

(**a**) (**b**)

Figure 4. Influence of the flexoelectric parameter r_1 on the gain coefficient. (**a**) $p = L$, (**b**) $p = L/4$; $r_1 = 1$ (solid), 2 (dashed), 3 (dot-dashed); $r_2 = -3$.

In our theory, beams coupling and gain of the signal beam are determined by the interaction of the photorefractive field with the LC flexopolarization $\mathbf{P}_f = e_1\mathbf{n}\nabla \cdot \mathbf{n} + e_3(\nabla \times \mathbf{n} \times \mathbf{n})$, where the first and second terms are connected with the splay and bend director deformations, respectively [17]. It is of interest to clarify the role of these director deformations in the case of the nematic and cholesteric type behavior of the gain coefficient. For this, we study the influence of the flexoelectric coefficients e_1 and e_2 on the gain, where the flexoelectric coefficient e_1 is responsible for the contribution of the splay director deformation and the flexoelectric coefficient e_3 is responsible for the contribution of the bend director deformation.

Influence of the coefficients e_1 and e_3 on the gain coefficient is shown, respectively, in Figure 5a,b for the case $p = L$ when the nematic character of the gain coefficient behavior takes place. It can be seen that in the entire region of the grating spacing, which is usually used in experimental measurements, the contributions from the splay and bend director deformations are of the same sign and comparable. For two-beam energy exchange in the nematic LC, only the sum of the flexoelectric coefficients, $e_1 + e_3$, appears [12] and is consistent with this theoretical approach.

For the cholesteric case ($p = L/4$), the influence of the coefficients e_1 and e_3 on the gain coefficient is shown in Figure 6a,b, respectively. Comparing Figure 6a,b we can see that in this case the contributions from the splay and bend director deformations are comparable and have the same sign only at small grating spacings. At larger grating spacings, the contribution from the bend director deformation has the opposite sign and prevails, providing the observable cholesteric behavior of the gain coefficient, which is again consistent experimentally.

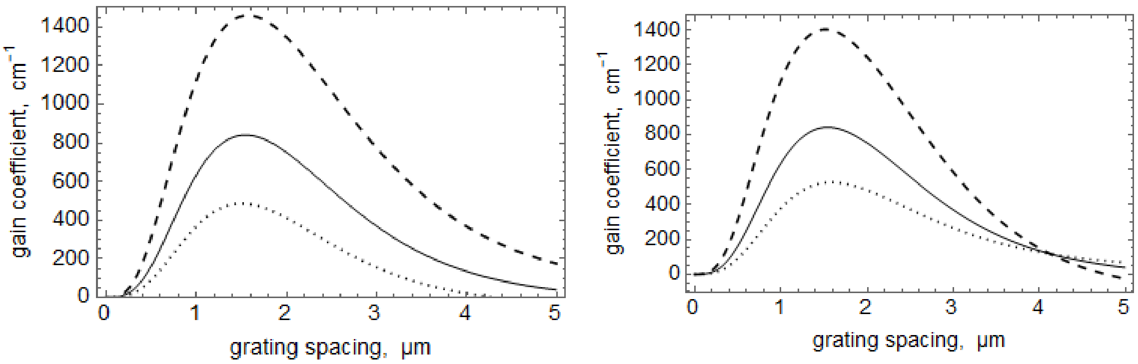

(**a**) (**b**)

Figure 5. Influence of the splay and bend director deformations on the gain coefficient at $p = L$. (**a**) $e_1/K = 0.1$ (dotted), 1 (solid), 3 (dashed), $e_3/K = 1$; (**b**) $e_3/K = 0.1$ (dotted), 1 (solid), 3 (dashed), $e_1/K = 1$.

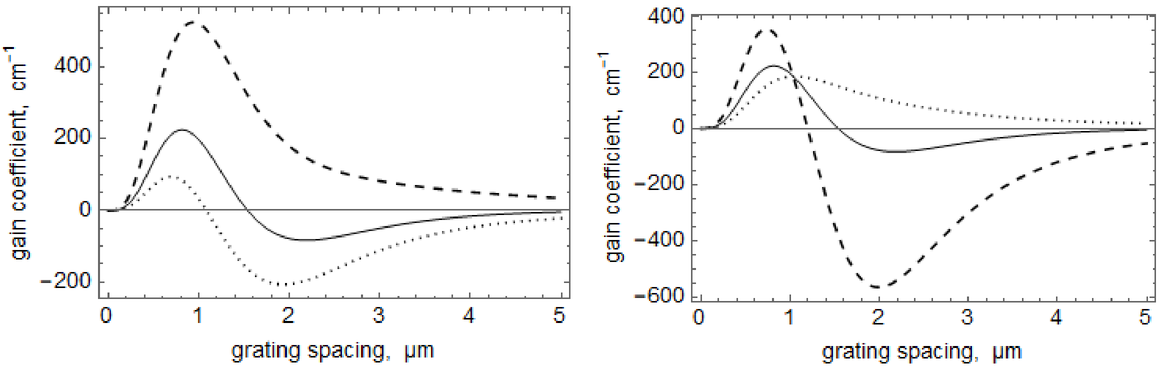

(**a**) (**b**)

Figure 6. Influence of the splay and bend director deformations on the gain coefficient at $p = L/4$. (**a**) $e_1/K = 0.1$ (dotted), 1 (solid), 3 (dashed), $e_3/K = 1$; (**b**) $e_3/K = 0.1$ (dotted), 1 (solid), 3 (dashed), $e_1/K = 1$.

5. Conclusions

The dependence of the signal beam gain coefficient on the director grating spacing, $\Gamma(\Lambda)$, observed in the cholesteric LC, can arise in the LC cell with the director twisting only when the flexoelectric parameter r_2 is negative. For typical parameters of hybrid LC cells used experimentally for two-beam energy exchange, the cholesteric type of $\Gamma(\Lambda)$ can appear when the director helix pitch becomes smaller than the cell thickness. If the parameter r_2 is positive, the gain coefficient dependence on the director grating spacing at any cholesteric pitch has a character observed in the nematic LC. For small director twisting such that the director helix pitch noticeably exceeds the cell thickness, the influence of the parameter r_2 on the gain coefficient becomes negligibly small. Value of the flexoelectric parameter r_1 does not influence the character of the gain coefficient dependence $\Gamma(\Lambda)$; however, the extremes of $\Gamma(\Lambda)$ increase with increasing r_1.

When the dependence $\Gamma(\Lambda)$ is of the nematic type the contributions into the gain coefficient from the splay and bend director deformations have the same sign and are comparable in all intervals of the grating spacing Λ. In the case of the cholesteric type of $\Gamma(\Lambda)$, the contributions from the splay and bend director deformations are comparable and have the same sign only at small grating spacings. At larger grating spacings, the contribution from the bend director deformation has the opposite sign and prevails, providing the observable cholesteric behavior of the gain coefficient.

Author Contributions: Conceptualization and methodology, V.Y.R.; Investigation and writing—original draft preparation, I.P.P.; Formal analysis, M.E.M.; Validation, J.E.S.; Writing—review and editing, supervision, D.R.E. All authors have read and agreed to the published version of the manuscript.

Funding: This research was funded by STCU, grant number P649a.

Conflicts of Interest: The authors declare no conflict of interest. The funders had no role in the design of the study; in the collection, analyses, or interpretation of data; in the writing of the manuscript, or in the decision to publish the results.

References

1. Solymar, I.; Webb, D.J.; Grunnet-Jepsen, A. *The Physics and Applications of Photorefractive Materials*; Clarendon Press: Oxford, UK, 1996.
2. Cook, G.; Finnan, C.J.; Jones, D.C. High optical gain using counterpropagating beams in iron and terbium-doped photorefractive lithium niobate. *Appl. Phys. B Lasers Opt.* **1999**, *68*, 911–916. [CrossRef]
3. Wiederrecht, G.P.; Yoon, B.A.; Wasielewski, M.R. High photorefractive gain in nematic liquid crystals doped with electron donor and acceptor molecules. *Science* **1995**, *270*, 1794–1797. [CrossRef]
4. Khoo, I.C.; Guenther, B.D.; Wood, M.V.; Chen, P.; Shih, M.-Y. Coherent beam amplification with a photorefractive liquid crystal. *Opt. Lett.* **1997**, *22*, 1229–1231. [CrossRef] [PubMed]
5. Ono, H.; Kawatsuki, N. High-performance photorefractivity in high- and low-molar-mass liquid crystal mixtures. *J. Appl. Phys.* **1999**, *85*, 2482–2487. [CrossRef]
6. Parka, J.; Kowerdziej, R.; Romaniuk, M. Photorefractive properties of new liquid crystals in the near-infrared range. *Liq. Cryst.* **2011**, *38*, 25–30. [CrossRef]
7. Cook, G.; Carns, J.L.; Saleh, M.A.; Evans, D.R. Substrate Induced pre-tilt in hybrid liquid crystal/inorganic photorefractives. *Mol. Cryst. Liq. Cryst.* **2006**, *453*, 141–153. [CrossRef]
8. Sutherland, R.L.; Cook, G.; Evans, D.R. Determination of large nematic pre-tilt in liquid crystal cells with mechanically rubbed photorefractive Ce: SBN windows. *Opt. Express* **2006**, *14*, 5365–5375. [CrossRef] [PubMed]
9. Evans, D.R.; Cook, G. Bragg-matched photorefractive two-beam coupling in organic–inorganic hybrids. *J. Nonlinear Opt. Phys. Mater.* **2007**, *16*, 271–280. [CrossRef]
10. Evans, D.R.; Cook, G.; Reshetnyak, V.Y.; Liebig, C.M.; Basun, S.A.; Banerjee, P.P. *Photorefractive Organic Materials and Applications*; Blanche, P.-A., Ed.; Springer: Cham, Switzerland, 2016; pp. 223–247.
11. Herrington, M.; Daly, K.; Buchnev, O.; D'Alessandro, G.; Kaczmarek, M. AC-field–enhanced beam coupling in photorefractive, hybrid liquid crystals. *EPL* **2011**, *95*, 14003. [CrossRef]
12. Reshetnyak, V.Y.; Pinkevych, I.P.; Cook, G.; Evans, D.R.; Sluckin, T.J. Two-beam energy exchange in a hybrid photorefractive-flexoelectric liquid-crystal cell. *Phys. Rev. E* **2010**, *81*, 031705. [CrossRef] [PubMed]
13. Reshetnyak, V.Y.; Pinkevych, I.P.; Cook, G.; Evans, D.R.; Sluckin, T.J. Two-beam energy exchange in a hybrid photorefractive inorganic-cholesteric cell. *Mol. Cryst. Liq. Cryst.* **2012**, *560*, 8–22. [CrossRef]
14. Reshetnyak, V.Y.; Pinkevych, I.P.; Sluckin, T.J.; Cook, G.; Evans, D.R. Beam coupling in hybrid photorefractive inorganic- cholesteric liquid crystal cells: Impact of optical rotation. *J. Appl. Phys.* **2014**, *115*, 103103. [CrossRef]
15. Tabiryan, N.V.; Umeton, C. Surface-activated photorefractivity and electro-optic phenomena in liquid crystals. *JOSA B* **1998**, *15*, 1912–1917. [CrossRef]
16. Jones, D.C.; Cook, G. Theory of beam coupling in a hybrid photorefractive-liquid crystal cell. *Opt. Commun.* **2004**, *232*, 399–409. [CrossRef]
17. De Gennes, P.G.; Prost, J. *The Physics of Liquid Crystals*, 2nd ed.; Clarendon Press: New York, NY, USA, 1993; p. 268.
18. Kogelnik, H. Coupled wave theory for thick hologram gratings. *Bell Syst. Tech. J.* **1969**, *48*, 2909–2947. [CrossRef]
19. Yeh, P. *Introduction to Photorefractive Nonlinear Optics*; Wiley: New York, NY, USA, 1993; p. 89.
20. Jarem, J.M.; Banerjee, P.P. *Computational Methods for Electromagnetic and Optical Systems*, 2nd ed.; CRC Press: New York, NY, USA, 2011; Chapter 6.
21. Blinov, L.M.; Barnik, M.I.; Ohoka, H.; Ozaki, M.; Shtykov, N.M.; Yoshino, K. Surface and flexoelectric polarization in a nematic liquid crystal 5CB. *Eur. Phys. J. E* **2001**, *4*, 183–192. [CrossRef]

22. Edwards, E.G.; Brown, C.V.; Kriezis, E.E.; Elston, S.J. Behaviour of a nematic liquid crystal cell containing a diffraction grating. *Mol. Cryst. Liq. Cryst.* **2003**, *400*, 13–19. [CrossRef]
23. Morris, S.M.; Clarke, M.J.; Blatch, A.E.; Coles, H.J. Structure-flexoelastic properties of bimesogenic liquid crystals. *Phys. Rev. E* **2007**, *75*, 041701. [CrossRef] [PubMed]
24. Le, K.V.; Araokaa, F.; Fodor-Csorbab, K.; Ishikawa, K.; Takezoe, H. Flexoelectric effect in a bent-core mesogen. *Liq. Cryst.* **2009**, *36*, 1119–1124.